Modelling transport in submicron structures using the relaxation time Boltzmann equation

1991 J. Phys.: Condens. Matter 3 9447

(http://iopscience.iop.org/0953-8984/3/47/016)

J. Phys.: Condens. Matter 3 (1991) 9447–9458. Printed in the UK

Modelling transport in submicron structures using the relaxation time Boltzmann equation

Bernard J Geurts†
Philips Research Laboratories, PO Box 80 000, 5600 JA Eindhoven, The Netherlands

Received 21 May 1991, in final form 19 August 1991

Abstract. We present a systematic evaluation of transport properties of semiconducting submicron structures as predicted by computer simulations based on the Boltzmann equation. The influence of variations in the relaxation time of the collision process and the geometry of a model n^+nn^+-diode are studied. Both ballistic and non-ballistic situations are considered and compared to approximating moment models. Already small ballistic effects, showing up as non-uniform features in the high velocity behaviour of the distribution function, cause considerable error in the moment model predictions for the I–V characteristics.

1. Introduction

Transport properties of semiconducting submicron structures have received increasing attention over the last few years. New phenomena come to dominate these properties as sizes are reduced further and high mobility materials become available for future device applications [1–7]. Far from equilibrium effects, e.g. hot and ballistic electron transport as well as large gradients in the electric field and the electron density, become more important. Typically, these effects are dominant in small regions of the structures, whereas in other regions near equilibrium conditions are observed. A wide range of relevant typical scales is found simultaneously in predominantly ballistic situations, i.e. both rapid and slow variations in the distribution function are observed in different regions of the devices and different velocity regions. By studying the Boltzmann equation, in the relaxation time representation, we show how ballistic effects depend on the relaxation time and the geometry parameters of a model n^+nn^+-diode. Our calculations directly clarify the failure of lower order moment equation models for predominantly ballistic transport conditions [6,7]. In these models one needs to truncate the hierarchy of moment equations by making an assumption on the form of the distribution function, which is usually of 'Maxwellian' type [4,5,7]. The actual distribution function found in direct evaluation of the Boltzmann equation greatly differs from this assumed reference form in the ballistic domain. In the non-ballistic ('diffusive') regime the essential features of the distribution function can quite well be captured with a small number of typical scales, e.g. based upon the local 'drift velocity' and 'electron temperature' only. The assumed 'Maxwellian' form for the

† Present address: Twente University, Department of Applied Mathematics, PO Box 217, 7500 AE Enschede, The Netherlands.

0953-8984/91/479447+12$03.50

distribution function resembles the actual distribution function to a greater extent and the corresponding model predictions agree much better with the Boltzmann results. Through the use of a new numerical integration method for the Boltzmann equation, based on the method of characteristics, and a proper evaluation of the singularities present for small velocities/electric fields, precise evaluation has become possible for a wide range of parameters [8].

The approach taken in this paper implies that we *do not* attempt a full microscopic simulation of the transport properties. We use the Boltzmann equation in one velocity and one spatial dimension, with a relaxation time representation for the collision integral. With this approach, we overestimate ballistic effects and focus in this extreme test case on the impact of 'ballisticity' on various low order moments [1]. Collision integrals can be treated more realistically with Monte Carlo simulations [2], which can accurately describe microscopic phase space transport phenomena. However, the large number of (partially) adaptable and unknown parameters appearing in such calculations, seriously restricts a clear separation between the various physical effects included and their influence on the predictions of low order moments. The present study oversimplifies the collision processes and allows for a clear interpretation of the effects observed in the predicted moments in terms of the appearence and extent of ballistic effects. Specific trends in the properties can be studied in a more flexible way than possible with more refined Monte Carlo simulations. A direct, numerically exact, evaluation of the full distribution function is obtained; no additional approximations are introduced. Hence, it furnishes a genuine testing ground for approximating schemes which should have the potential to be both adaptable to more complex geometries and to give accurate predictions over a wide range of parameters, maintaining a transparent physical content. The failure of low order moment models to represent the relevant aspects of ultra-small devices calls for the construction of such alternative approximating descriptions. It is still an open matter in what way new (simple) approximating schemes should be realized.

In section 2 we present the Boltzmann equation and give an overview of the numerical approach. Section 3 is devoted to a discussion of simulation results obtained for the distribution function and low order moments, concentrating on the influence of the relaxation time and the geometry of the model diode. Finally, in section 4 we compare these predictions with those generated with simple approximate low order moment models and summarize our findings.

2. Boltzmann equation approach

We introduce the spatially inhomogeneous Boltzmann equation. The hierarchy of corresponding moment equations approximating this Boltzmann equation will be presented and closing relations indicated. Then we briefly describe the numerical procedure adopted to evaluate this model.

The classical description of electron transport through solids is based on the interplay between the Boltzmann equation and Poisson's equation. The Boltzmann equation governs the distribution function $f(r, v)$ and, in one spatial- and velocity dimension, it can be expressed as [1]

$$\{v\partial_r - E(r)\partial_v\}f(r,v) = -\frac{1}{\tau}\{f(r,v) - f_0(r,v)\} \tag{2.1}$$

where we adopt the parabolic band approximation and assume a relaxation time representation (with rate τ) for the collision term and f_0 represents the local equilibrium distribution function. Hence, in (2.1) electrons are driven out of (local) equilibrium under the action of the electric field (E) present in the device and upon scattering are sent back/thermalize with rate τ to a state of local equilibrium, corresponding to f_0. We concentrate on electrons only, which is an adequate assumption for n^+nn^+-diodes in which transport by holes can be neglected. We use scaled variables, i.e. position r and velocity v are measured in units r_0 (the Debye length) and v_0 (the thermal velocity) respectively where

$$r_0 = \left(\frac{\varepsilon k_B T_0}{e^2 M_{ref}}\right)^{1/2} \qquad m^* v_0^2 = k_B T_0 \tag{2.2}$$

with the understanding that k_B is Boltzmann's constant, T_0 the lattice temperature, ε the permittivity, e the unit of charge, m^* the effective mass and M_{ref} a reference particle density in the system. Both f and f_0 are in units M_{ref}/v_0. This equation represents the balance between local flow of probability in phase space of charged particles in an associated electric field and transport of probability due to scattering processes. The electric field E is measured in units $E_0 \equiv (m^* v_0^2)/(e r_0)$. It is determined by Poisson's equation:

$$d_{rr}\Psi(r) = M_0(r) - C(r) \qquad E = -d_r\Psi \tag{2.3}$$

where $C(r)$ describes the doping profile of the device and M_0 the electron density, in units M_{ref}. Throughout we adopt the notation M_0 (instead of e.g. n or ρ as elsewhere in literature) for the (scaled) electron density in order to make the connection with higher order moments of f, to be introduced momentarily, more transparent. The model n^+nn^+-diode is represented by the following doping profile:

$$C(r) = \begin{cases} C_+ & 0 \leqslant r \leqslant d_1 \qquad d_2 \leqslant r \leqslant l \\ C_- & d_1 < r < d_2 \end{cases} \tag{2.4}$$

in which C_+ is the doping concentration in the n^+-regions, C_- the (minority) doping concentration in the n-region, l the length of the total structure and $d \equiv d_2 - d_1$ the width of the n-region. Typically $C_- \ll C_+$ and combination with the abruptness of the doping profile implies large electric fields and rapid exponential variations in the electron density in regions close to the doping steps.

A similar model was first introduced by Baranger and Wilkins. Several basic assumptions are implied by the above formulation and we refer the reader to [1,9] for a detailed discussion. We stress that the spatially inhomogeneous Boltzmann equation is adopted as a calculational model overestimating ballistic effects. In this way we concentrate on a 'worst case' model situation to clarify the influence of ballistic transport on low order moments. Moreover, the situations giving rise to ballistic effects can be monitored. The simplicity of this approach implies greater flexibility in investigating specific trends as a function of parameters. Furthermore, rapid local variations caused by the abrupt doping profile lead to serious numerical stability problems which seem intractable with more realistic scattering terms if one maintains a direct evaluation of the equation rather than a Monte Carlo simulation approach.

In device simulations one usually concentrates on low order velocity moments of the distribution function; the mth moment M_m is defined as $M_m \equiv \langle v^m \rangle$, $m = 0, 1, 2, \ldots$. To clarify these moments; M_0 is proportional to the electron density, M_1 to the current density, M_2 to the kinetic energy density, M_3 to the current in the kinetic energy density, etc. Moreover, combinations of lower order moments are readily interpreted; the ratio of M_1 and M_0 is proportional to the drift velocity, a combination of $M_0, \ldots, M_2$ can be related to the electron temperature etc. The set of moments $\{M_m(r)\}$ obeys [7]

$$d_r M_{m+1} + mEM_{m-1} = -\frac{1}{\tau}\{M_m - M_{m,0}\} \qquad m = 0, 1, 2, \ldots \tag{2.5}$$

which is readily derived from (2.1) by multiplying both sides with v^m and (partial) integration over all v. The local equilibrium distribution function appearing in (2.1) can be expressed as

$$f_0(r, v) \equiv \frac{M_0(r)}{\sqrt{2\pi}} \exp\left(-\frac{v^2}{2}\right). \tag{2.6}$$

This implies that the reference moments $\{M_{m,0}\}$ are given by

$$M_{2m,0} = M_0 \prod_{j=1}^{m} (2j - 1) \qquad M_{0,0} = M_0 \tag{2.7}$$

and $M_{2m+1,0} = 0$. The mth moment is governed in part by the spatial derivative of the $(m + 1)$th moment. Hence, a closing relation must be postulated expressing a higher order moment in terms of lower order moments. With such a closing relation the system of equations (2.5) is finite and can be treated numerically yielding approximate predictions for the moments. The accuracy of such an approach heavily depends on the truncation order and the exact closing relation used. Such closing relations are frequently generated with some assumed form for the distribution function as basis [4, 5, 7]. There is no *a priori* justification for the use of a particular choice other than related (semi) empirical considerations. The justification for a specific choice is mostly given afterwards and related to the accuracy of a particular prediction in relation to experiments or more refined model calculations. As such, the strict physical predictive power is limited. The numerical Boltzmann simulation results will be compared with a two- (i.e. drift-diffusion) and a four-moment model. The closing relations are obtained from an expansion of the distribution function around a pure Maxwellian distribution function in Hermite polynomials [4]. In particular, the 'drift-diffusion' (i.e. two moments) closing relation used is $M_2 = M_0$, i.e. assuming equilibrium between electrons and phonons by taking the electron temperature equal to the lattice temperature, and the four-moment closing relation is taken as $M_4 = 6M_2 - 3M_0$. A more detailed discusion may be found in e.g. [5, 7]

In order to complete the above model, we need to specify boundary conditions. Throughout, we consider n^+nn^+-diodes with doping banks (i.e. the n^+-regions) wide enough such that at $r = 0$ and $r = l$ the spatially homogeneous situation applies to close approximation. In that case the electron density at the boundaries equals the doping concentration in the n^+-region and the Boltzmann equation reduces to

$$-E_b \partial_v f_b(v) = -\frac{1}{\tau}\{f_b(v) - f_{0,b}(v)\} \tag{2.8}$$

where the subscript b denotes that we consider the boundary. Since the total charge distribution is considered neutral, the electric field at the boundaries is equal, and the above holds at both boundaries. One readily solves for f_b and obtains:

$$f_b(v) = \begin{cases} \frac{\delta}{2}\exp\left(\delta\left\{\frac{\delta}{2}-v\right\}\right)\operatorname{erfc}\left(\frac{\delta-v}{\sqrt{2}}\right) & \delta > 0 \\ -\frac{\delta}{2}\exp\left(\delta\left\{\frac{\delta}{2}-v\right\}\right)\operatorname{erfc}\left(\frac{v-\delta}{\sqrt{2}}\right) & \delta < 0 \end{cases} \tag{2.9}$$

in which $\delta = -1/(\tau E_b)$. Special care must be paid to $|\delta|$ much larger and much smaller than 1, in which case asymptotic expansions should be used. Notice that f_b can be evaluated if E_b is known. In addition, the boundary conditions for Ψ are taken as $\Psi(0) = 0$ and $\Psi(l) = V$ in which V denotes the (scaled) applied voltage.

We next briefly describe the self-consistent numerical approach used to evaluate the above model. The central method for solving the Boltzmann part is based on the method of characteristics in which we assume the electric field E to be known for the moment. As a consequence of this, the family of characteristics, given implicitly by $(v^2/2) - \Psi(r) = \alpha$, where α is a constant, is also assumed known. If f is desired in a point (r, v) one first reconstructs the specific member of this characteristics family, by evaluation of the corresponding α, on which this point is located. Then one integrates the Boltzmann equation along this characteristic, starting at the ('upstream') boundary, i.e. at $r = 0$ if $v > 0$ and at $r = l$ if $v < 0$. The value of f at this boundary is given by (2.9) evaluated at the boundary point corresponding to the specific characteristic selected. If that characteristic does not connect to any boundary point one determines $f(r, v)$ through repeated integration along the closed characteristic (which in such a case lies completely within the region in which the calculation is performed) and requires the distribution function to be single valued. In this way one may determine f, given an electric field E, at any point (r, v). Updating the electron density and solving Poisson's equation for this new density completes one step in the full iteration. Repeated application of the above yields a (slowly) converging iteration process which is repeated until convergence is obtained. The iteration is stopped if the maximal relative error in Ψ and M_0 is smaller than some tolerance. A detailed description of the above scheme will be presented elsewhere [8]. Here, we concentrate on the results obtained with the above, direct integration algorithm and turn to the predictions for the distribution function and low order moments in the next section.

3. Ballistic and non-ballistic predictions for an n^+nn^+-diode

In this section we present Boltzmann predictions for low order moments as depending on the relaxation time (τ) and the width of the n-region (d) for various applied voltages. Both non-ballistic ('small' τ and/or 'large' d) and ballistic situations will be considered. First, however, we present simulation results for the distribution function itself, showing the appearence of sharp high velocity peaks in the distribution function, next to a more familiar 'bell'-shaped form at lower velocities as we enter the ballistic domain, e.g. through an increase in τ.

We consider a GaAs based diode with $m^* = 0.069 m_e$ (m_e being the electron rest mass), $\varepsilon_r = 12.5$, an n-width of 10^{-7}–10^{-6} m and a total length l of 10^{-6}–10^{-5} m.

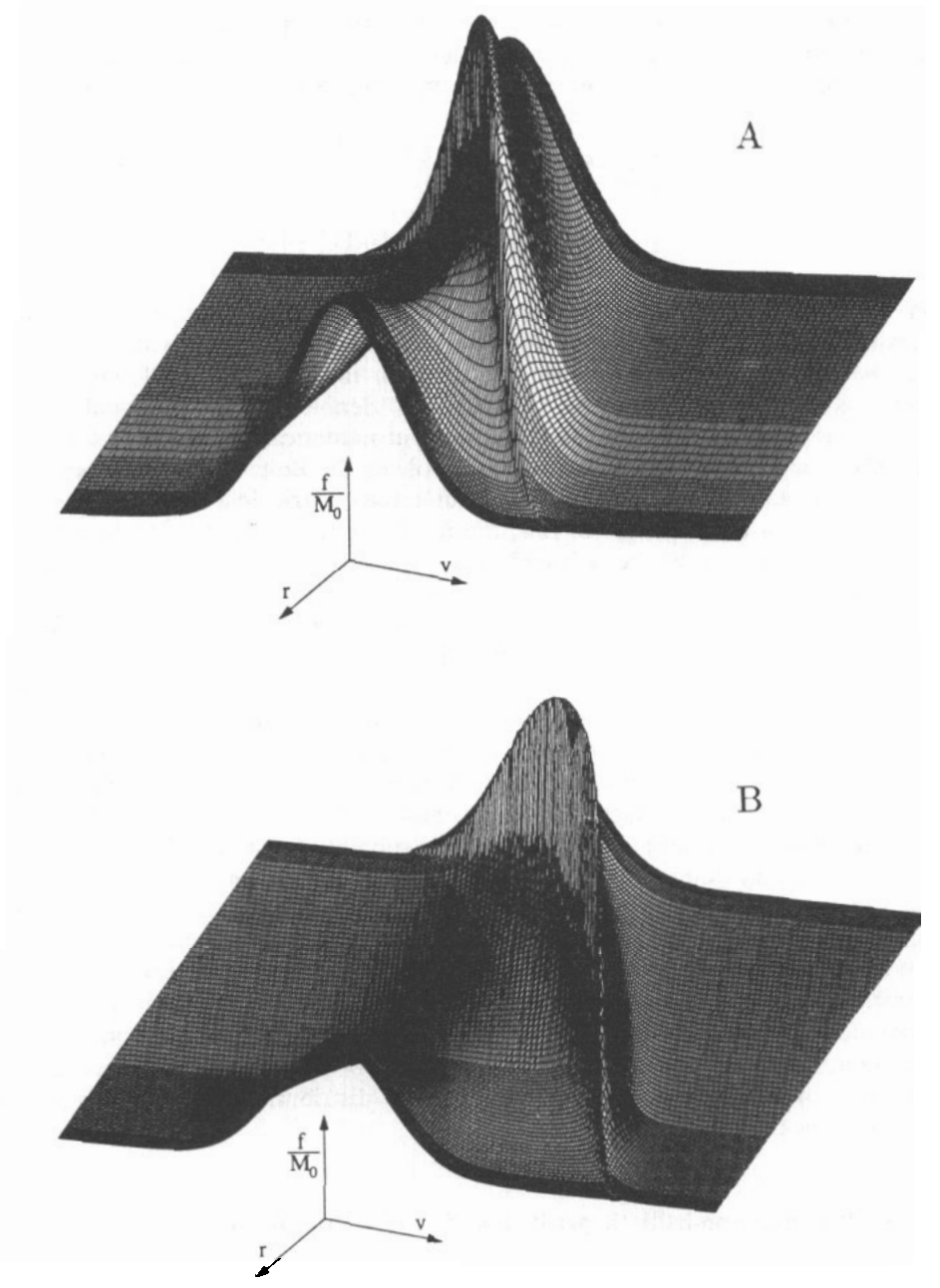

Figure 1. Perspective plot of $f(r, v)/M_0(r)$ with $\tau = 5 \times 10^{-13}$ s, and n-width $d = 0.4 \times 10^{-6}$ m, a total length $l = 4.4 \times 10^{-6}$ m and applied voltages $V = 0.1$ V (*a*); $V = 0.3$ V (*b*). The displayed part of position space is the low doping region between $r = d_1$ (in the back) and $r = d_2$ (in the front).

Doping concentrations are taken as $C_+ = 10^{24}$ m^{-3} and $C_- = 2 \times 10^{21}$ m^{-3} (the reference density M_{ref} is fixed to C_+). The relaxation time will be in the range 10^{-13}–10^{-14} s, and the lattice temperature $T_0 = 300$ K. For a more detailed description of

the choice of these parameter regions we refer to [1, 9].

In figure 1 we show the distribution function at parameters corresponding to the predominantly ballistic regime showing the influence of an increased applied voltage. Only the segment corresponding to the n-region is shown. One clearly recognizes the ('drifted') Maxwellian shape (roughly speaking) of f at the doping interfaces, i.e. at $r = d_1$ and $r = d_2$. Notice that $r = d_1$ corresponds to the 'back part' of the figure and $r = d_2$ to the 'front part'. As the electrons enter the n-region they are first slowed down on the average, corresponding to a somewhat higher and sharper distribution function (i.e. 'cooling' to which we turn momentarily). The electrons move up a potential barrier related to the electrostatic potential, in the 'first' part of the n-region. After this initial step, the electrons get accellerated, which is clearly represented by the high velocity ballistic 'ridge' shown. As we enter further into the n-region, gradually more and more electrons get thermalized, i.e. scattered back to the local equilibrium state and at $r = d_2$ virtually all ballistic electrons have disappeared and we have returned to the situation at $r = d_1$ to close approximation. An increase in the applied voltage favours these effects. At $V = 0.1$ V the fraction of electrons moving ballistically is roughly the same as the amount of 'lower' velocity electrons. However, at $V = 0.3$ V, the ballistic electrons heavily outweigh the 'lower' velocity electrons for certain values of r. In figure 2 we plotted the electrostatic potential in which the electrons move, displaying the different regions of transport discussed above. The high built-in electric fields observed in this diode imply that far from equilibrium conditions are reached with great ease. So, small applied voltages cause quite large ballistic effects at appropriate parameter values.

In order to obtain a quantitative overview, we plotted 'cross-sections' of f as a function of velocity at a number of points within the structure. As shown above, an increase in V favours ballistic effects, as does an increase in the relaxation time τ. In figures 3–5 we show f at $V = 0.25$ at the r-values as indicated by 'plusses' in figure 2 and for three different τ values. A decrease in τ corresponds to a (sharp) decrease in the amount of electrons moving ballistically within the n-region, at the same applied voltage. In the ballistic cases (figures 3 and 4) one observes a definite cooling effect, i.e. a much narrower distribution function as the electrons move up the potential barrier. Deeper within the n-region a sharp ballistic peak develops which disappears almost completely when approaching the second doping step. The fraction of ballistic electrons sharply decreases as τ is decreased, and at $\tau = 1 \times 10^{-13}$ s almost no ballistic effects are noticed (cf. figure 5). A similar observation can be made with respect to variations in the width of the n-region, d. As d is decreased far enough (depending on τ), predominantly ballistic transport is observed in the n-region of the diode. There is a sharp 'cross-over' from non-ballistic to predominantly ballistic transport in this structure as a function of τ and d. Roughly speaking, as ballistic electrons (with velocity on the order of d/τ or higher) start to represent a non-neglegible fraction ($\approx$ a few percent of more) of the total ensemble of electrons the dominant physical transport phenomena change rapidly from 'diffusive' to 'ballistic'.

The 'cooling' and 'heating' of the electrons in the n-region is shown in figure 6 in which we represent the effect of an applied voltage. The electron temperature (T_e) is defined as

$$T_e = T_0 \frac{M_2 M_0 - M_1^2}{M_0^2} \tag{3.1}$$

and is related to the 'width' of the distribution. Both 'cooling' and 'heating' are

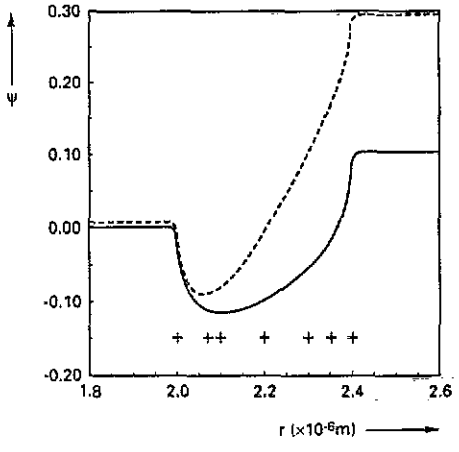

Figure 2. Plot of Ψ as a function of position, with parameters as in figure 1. The full curve corresponds to $V = 0.1$ and the dashed curve to $V = 0.3$. Also shown are the positions used to generate the distribution function f as in figures 3–5 (marked by 'plusses' and labelled 1...7 for later convenience). The n-region is situated between d_1 and d_2.

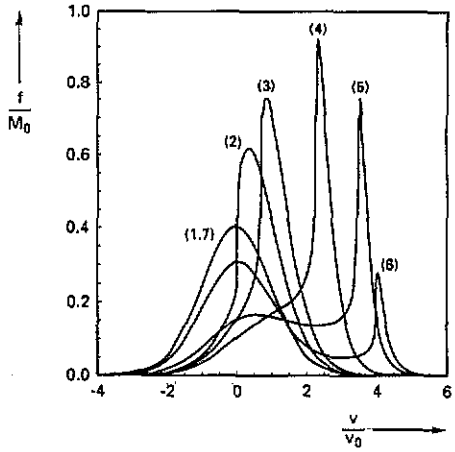

Figure 3. Plot of $f(r, v)/M_0(r)$ at $V = 0.25$ V and the same parameters as in figure 1. We show results at $r = 2$ (labelled 1); $r = 2.06875$ (labelled 2, here Ψ has its minimal value); $r = 2.1$ (labelled 3); $r = 2.2$ (labelled 4); $r = 2.3$ (labelled 5) ; $r = 2.35$ (labelled 6) and $r = 2.4$ (labelled 7). All these positions are in units 10^{-6} m.

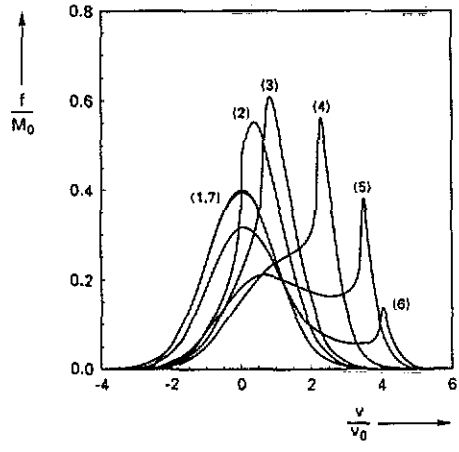

Figure 4. Plot of $f(r, v)/M_0(r)$ at $V = 0.25$ V and the same parameters as in figure 1, but $\tau = 2.9 \times 10^{-13}$ s. The curve labelling is the same as in figure 3.

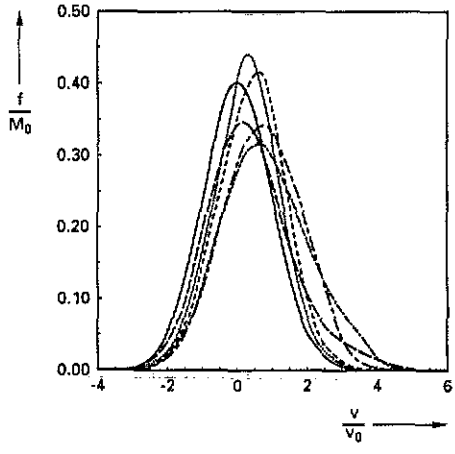

Figure 5. Plot of $f(r, v)/M_0(r)$ at $V = 0.25$ V and the same parameters as in figure 1, but $\tau = 1 \times 10^{-13}$ s. We show results at $r = 2$ (full curve); $r = 2.06875$ (dotted curve, here Ψ has its minimal value); $r = 2.1$ (dashed curve); $r = 2.2$ (chain dotted curve); $r = 2.3$ (long chain-dashed curve) and $r = 2.35$ (long dashed curve). All these positions are in units 10^{-6} m.

clearly recognized, and an increase in the applied voltage increases these effects. The 'heating' of the electrons is influenced to a greater extent than the 'cooling', which

is due to the fact that the potential barrier close to $r = d_1$ changes less than the potential difference between the doping steps. Finally, in figure 7 we show the kinetic energy density current, defined as $Q = (m^* v_0^3 M_{\text{ref}} M_3)/2$, displaying variations in the relaxation time. Two distinct peaks are recognized close to the doping interfaces, which become more pronounced as the relaxation time increases, i.e. if ballistic effects become more important. The upper two curves correspond (roughly speaking) to the ballistic regime, whereas the lower two correspond to the non-ballistic regime. The features of Q in these two regimes are quite different; in the ballistic regime the peaks in Q are both higher and wider in comparison to the non-ballistic results. A study of the influence of d shows similar effects; a decrease in d implies situations further separated from local equilibrium.

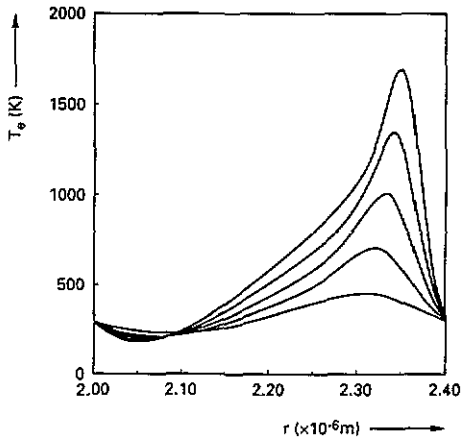

Figure 6. Plot of the electron temperature (T_e) as a function of position using the same parameters as in figure 1, with $\tau = 2.9 \times 10^{-13}$ s. Applied voltages used in this calculation are $V = 0.5$ V (largest cooling and heating) and decreasing with steps of 0.1 V.

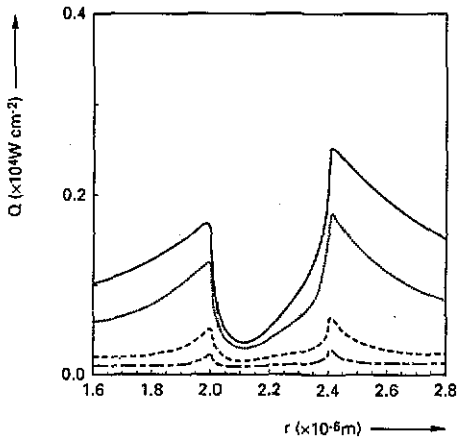

Figure 7. Plot of the kinetic energy density current (Q) as a function of position at $V = 0.1$ V showing the dependence on τ with parameters as in figure 1. We used $\tau = 5 \times 10^{-13}$ s (full curve); $\tau = 2.9 \times 10^{-13}$ s (dotted curve); $\tau = 1 \times 10^{-13}$ s (dashed curve) and $\tau = 5 \times 10^{-14}$ s (chain dotted curve).

4. Comparison with low order moment models

The hierarchy of moment equations needs to be closed by a relation expressing a high order moment in terms of lower order moments. The basis of such a closing relation is usually an assumption on the dominant form of the distribution function. The closing relations given in section 2 are obtained from an expansion of f around a Maxwellian distribution function. Improved expansions have been proposed corresponding to an expansion around 'drifted' and also 'drifted and heated' Maxwellians. In the first case the velocity is corrected with the drift velocity, and in the second case it is also scaled with the root of the local electron temperature. Complicated, nonlinear closing relations are obtained in the latter cases. The predictions of all these models, at any low truncation order (< 4) agree quite well with each other and

hence we only compare to the moment models corresponding to expansion around a pure Maxwellian [4,7]. Apparently, such an extension of the expansion functions is not able to bridge the large differences observed between the assumed and the actual distribution function. The accuracy of the predictions obtained with the moment models is correspondingly small, already in 'mildly' ballistic cases. We compare simulation results for low order moments as well as I–V characteristics and relate the failure of the moment models to the appearance of extra ballistic structure in the distribution function. The latter 'fine' structure in f can obviously not be covered with a Maxwellian type of expansion function. In addition, the homogeneous solution at the boundaries is also not exactly represented, which causes even moderate ballistic cases to be poorly predicted in some respects (e.g. the conductivity).

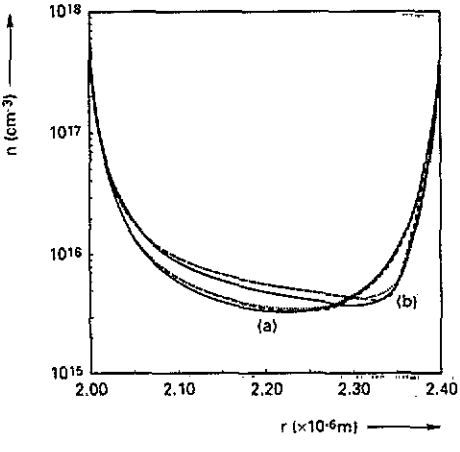

Figure 8. The electron density as a function of position at $\tau = 2.9 \times 10^{-13}$ s and $V = 0.1$ V (case a); $V = 0.5$ V (case b). The Boltzmann results are shown as full curves, the two-moments results as dotted curves and the four-moments results as dashed curves.

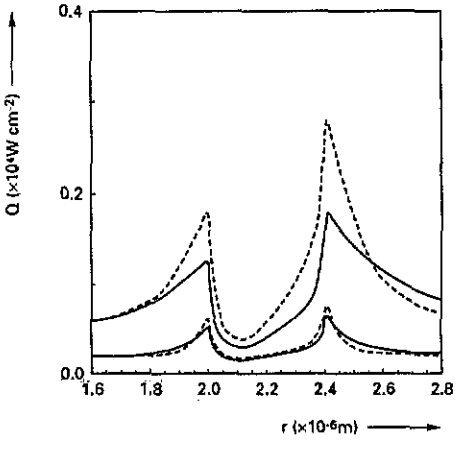

Figure 9. The kinetic energy denstiy current (Q) as a function of position at $V = 0.1$ V and $\tau = 1 \times 10^{-13}$ s (lower two curves); $\tau = 2.9 \times 10^{-13}$ s (upper two curves). The Boltzmann results are shown as full lines and the four-moments results as dashed lines. Parameters as in figure 1.

In figure 8 we plot the electron density as a function of position using $\tau = 2.9 \times 10^{-13}$ s and show the influence of an applied voltage. If V increases, both the two- and four-moment models give less accurate predictions of the electron density, though this quantity does not depend very sensitively on the presence of ballistic electrons. We also studied the effects of changes in τ and/or d. An increase in τ and/or a decrease in d implies a decrease of the range of applied voltages in which the moment predictions give acceptable representations of the actual electron density. Since the electron density is contained in the right hand side of all odd order moment equations (cf. (2.5) and (2.7)), small errors in the predictions have an influence on all other moments. Hence, the accuracy with which the electron density needs to be represented should be quite high in order to have reasonable accuracy in the higher order moments. The influence of these errors is largest in the odd order moments. Turning to figure 9 we notice that the four-moment prediction (dashed lines) of the kinetic energy density current (Q) becomes unacceptable already at small applied voltages if τ is large enough. We show results for Q at $V = 0.1$ V

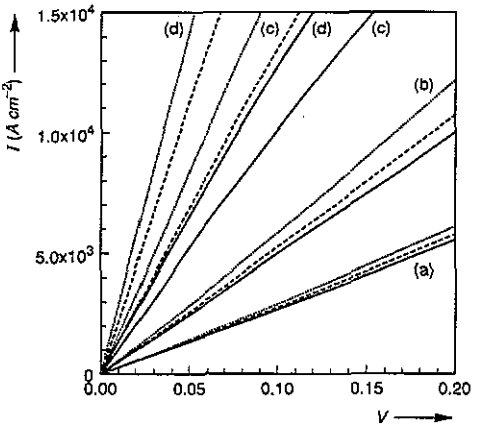

Figure 10. Comparison of the I–V characteristics as predicted by the two- and four-moments models with the corresponding Boltzmann results showing the influence of variations in the relaxation time τ, keeping d fixed to 0.4×10^{-6} m. The Boltzmann results are represented by the full curves, the two-moments results by the dotted curves and the four-moments results by the dashed curves. In the calculations τ was varied between $\tau = 5 \times 10^{-14}$ s (labelled a); 1×10^{-13} s (labelled b); 2.9×10^{-13} s (labelled c) and 5×10^{-13} s (labelled d). The other parameters are as in figure 1.

and $\tau = 1 \times 10^{-13}$ s ('non-ballistic'), $\tau = 2.9 \times 10^{-13}$ s ('mildly ballistic'). In the 'non-ballistic' case the prediction for Q roughly corresponds to the Boltzmann result, though the predicted peaks in Q are slightly too large and too sharp. In the ballistic case however, both the values as well as the global shape are predicted with large error.

A very strong influence of ballistic transport is seen in the I–V characteristics as predicted by the moment models in comparison with the Boltzmann results. In figure 10 we show such I–V characteristics for a wide range of τ values at $d = 0.4 \times 10^{-6}$ m. The applied voltage range is only moderate and the I–V curves shown exhibit all nearly linear dependence of I on V as reported elsewhere in literature, e.g. [1]. Only for very small τ values the predictions are roughly coincident and in this regime the improvements coming from the use of higher order moment models is virtually negligible. A decrease in d also results in less accurate predictions of the current since ballistic effects become more important. The use of higher order moment models provides a slight extension of the parameter region in which the predicted currents are still reasonably accurate. However, it is obvious that the predominantly ballistic regime can not be reached with any low order moment model [6,7]. Only the introduction of a (much) more complicated reference function, around which the expansions take place, seems to open the possibility to actually describe the ballistic regime properly, within a moment approach. It is not clear what guiding principles should be used in the construction of such a reference function and it is questionable whether such an approach would be applicable at all to more complex geometries.

References

[1] Baranger H U and Wilkins J W 1987 *Phys. Rev.* B **36** 1487

[2] Price P J 1979 *Semiconductors and Semimetals* vol 14, ed R K Willardson and A C Beer (New York: Academic) p 249
Jacoboni C and Reggiani L 1983 *Rev. Mod. Phys.* **55** 645
Moglestue C 1986 *IEEE Comput. Digital Tech.* **CAD-5** 326
Hess K 1988 *Advanced Theory of Semiconductor Devices* (Englewood Cliffs, NJ: Prentice-Hall)
Fischetti M V and Laux S E 1988 *Phys. Rev.* B **38** 9721
Sangiorgi E, Riccó V and Venturi F 1988 *IEEE Comput. Digital Tech.* **CAD-7** 259
[3] Cook R F and Frey J 1982 *IEEE Trans. Electron Devices* **ED-29** 970
Wang C T 1985 *Solid State Electron.* **28** 783
Hänsch W and Miura-Mattausch M 1986 *J. Appl. Phys.* **60** 650
Schöll E and Quade W 1987 *J. Phys. C: Solid State Phys.* **20** L871
Meinerzhagen B and Engl W L 1988 *IEEE Trans. Electron Devices* **ED-35** 689
Azoff E M 1988 *J. Appl. Phys.* **64** 2439
Stratton R 1962 *Phys. Rev.* **126** 2002
Blotekjaer K 1970 *IEEE Trans. Electron Devices* **ED-17** 38
[4] Bringer A and Schön G 1988 *J. Appl. Phys.* **64** 2447
[5] Portengen T, Boots H M J and Schuurmans M F H 1990 *J. Appl. Phys.* **68** 2817
[6] Geurts B J, Nekovee M, Boots H M J and Schuurmans M F H 1991 Exact and moment equation modeling of electron transport in submicron structures *Appl. Phys. Lett.* submitted
[7] Nekovee M, Geurts B J, Boots H M J and Schuurmans M F H 1991 Failure of extended moment equation approaches to describe ballistic transport in submicron structures *Phys. Rev.* B submitted
[8] Geurts B J 1991 Characteristics method for solving the spatially inhomogenous boltzmann equation *Philips Research Laboratories* in preparation
[9] Baranger H U 1986 *PhD Thesis* Cornell University